Solving nonlinear algebraic loops arising in input-saturated feedbacks

Franco Blanchini, Giulia Giordano, Francesco Riz, Luca Zaccarian

Solving nonlinear algebraic loops arising in input-saturated feedbacks

Franco Blanchini, *Senior Member, IEEE*, Giulia Giordano, *Senior Member, IEEE*, Francesco Riz, Luca Zaccarian, *Fellow, IEEE*

***Abstract*—We propose a dynamic augmentation scheme for the asymptotic solution of the nonlinear algebraic loops arising in well-known input saturated feedbacks typically designed by solving linear matrix inequalities (LMIs). We prove that the existing approach based on dynamic augmentation, which replaces the static loop by a dynamic one through the introduction of a sufficiently small time constant, works under some restrictive sufficient well-posedness conditions, requiring the existence of a diagonal Lyapunov matrix. However it can fail in general, even when the algebraic loop is well-posed. Then, we propose a novel approach whose effectiveness is guaranteed whenever well-posedness holds. We also show how this augmentation allows preserving the guaranteed region of attraction with Lyapunov-based designs, as long as a gain parameter is sufficiently large. We finally propose an adaptive version of the scheme where this parameter is adjusted online. Simulation results show the effectiveness of the proposed solutions.**

I. Introduction

Control of input-saturated plants, often denoted as bounded stabilization of dynamical systems, received much attention in the past 30-40 years from the nonlinear control community. For the special case of a linear plant, fundamental limitations have been characterized in the early work [1] and then constructive solutions have been given in [2], [3]. After those early works, the community started addressing optimality-based designs of bounded feedback stabilizers, wherein the whole control algorithm is designed, and anti-windup augmentations, where a filter is designed to augment an existing control scheme whose performance is undesirable for signals large enough to activate saturations. Comprehensive overviews of results in this area can be found in [4], [5], [6], [7].

An important milestone for providing optimality-based designs based on Linear Matrix Inequalities (LMIs) is given by [8], which showed for the first time that the use of an algebraic loop wrapped around the saturation nonlinearity can improve the transient response, especially in terms of directionality compensation with multi-input saturated plants. The pioneering work [8] did not formulate nor address well-posedness of the ensuing nonlinear algebraic loop (that is, existence and uniqueness of a solution of the ensuing nonlinear algebraic interconnection [9]). This was later done in [10], where sufficient well-posedness conditions were formulated and shown to structurally hold in the LMI-based designs of [8]. Interesting features associated with this nonlinear algebraic loop were also shown in [11] (see also [12]), where its solution was shown to be as hard as solving a quadratic program. Finally, [13] discussed certain fragilities associated with some of these loops, and [14] discussed a possible approach to ensuring a so-called "strong well-posedness" condition on the loop, partially addressing such fragilities.

In later years, building upon this sufficient condition, several stabilization and anti-windup schemes (see, e.g, [15], [16]) exploited the idea of designing optimality-based algebraic loops in saturated control schemes, even though their solution had only been partially discussed in [15, Remark 9], which suggests an approximate implementation algorithm, without proving why it is effective. Among other things, in this paper we prove the effectiveness of the algorithm in [15, Remark 9] when enforcing the above mentioned sufficient well-posedness conditions, but show that those solutions may be destabilizing in more general cases with well-posed algebraic loops.

A further understanding of the context was given in [17], where necessary and sufficient well-posedness conditions were given in terms of the determinants of certain matrices involving the feedback gain characterizing the algebraic loop. In later years, just a few methods have been given about how to solve these nonlinear algebraic loops in practical implementations, comprising the discussion in [7, §2.3.7], the method in [18, §4], which works under a diagonal dominance assumption, and the framework introduced in [19], where solving the algebraic loop is cast as a mixed linear complementarity problem, for which several iterative algorithms exist (as noted in [19, §5], these comprise projected iterative methods, interior point algorithms and pivoting schemes such as the Lemke algorithm). An explicit formula was also reported in [20, Lemma 3] (see also [21, Remark 2]), which only works for the single-input case. Nonetheless, the use of these algebraic loops in optimality-based saturated feedback design has persisted in later works, such as [22], [23], [24], [25], [26], [27], [28], [29], [30] and also [5, Ch. 7], by mostly relying on heuristics for their solutions (e.g., the Simulink algebraic loop solver),

Franco Blanchini acknowledges support by the Italian MIUR under Project 2017YKXYXJ, PRIN 2017.

Luca Zaccarian and Riccardo Bertollo are partially supported by the Agence Nationale de la Recherche (ANR) via grant Hybrid And Networked Dynamical sYstems (HANDY), number ANR-18-CE40-0010. Luca Zaccarian is also supported by the Italian Ministry for Research in the framework of the 2020 Program for Research Projects of National Interest (PRIN), under Grant 2020RTWES4 (DOCEAT).

F. Blanchini is with the Dipartimento di Scienze Matematiche Informatiche e Fisiche, University of Udine, Italy. Email: blanchini@uniud.it.

F. Riz is with the Department of Information Engineering and Computer Science, University of Trento, Italy. Email: francesco.riz@unitn.it.

G. Giordano and L. Zaccarian are with the Department of Industrial Engineering, University of Trento, Italy. Email: {giulia.giordano, luca.zaccarian}@unitn.it. L. Zaccarian is also with the LAAS-CNRS, Université de Toulouse, CNRS, Toulouse, France.

or on finite enumeration (see [7, §2.3.7]), which is effective when having a few input channels.

In this paper we solve asymptotically these nonlinear algebraic loops via a dynamic augmentation that is guaranteed to converge exponentially to the unique solution whenever the loop is well-posed. Our solution is based on the results of [31] and is shown to be effective whenever the necessary and sufficient conditions of [17] hold. We also revisit the solution suggested in [15, Remark 9] and we 1) show that it is not effective in general by way of an insightful counterexample; 2) prove its effectiveness whenever the sufficient conditions assumed in [15] are satisfied. This last proof is nontrivial and exploits the results of [32]. The dynamic augmentation that we propose falls into the category of dynamic inversion of nonlinear maps (see, e.g, the early works [33], [34] and references therein), which have been recently extended to a number of relevant scenarios (see, e.g., [31], [35], [36]), even though in our case the situation is quite peculiar due to the fact that the map under consideration is not differentiable, due to the Lipschitz nature of the saturation nonlinearity. Due to this fact, in our derivations, we rely on the use of Clarke's generalized gradients to prove our results.

The paper is organized as follows. In Section II we introduce the setup, background work and counterexamples illustrating the non-trivial nature of the problem at stake. In Section III we present and prove the properties of the mere solution of the nonlinear algebraic loop, while in Section IV we show how that same solution can be used to implement a dynamic augmentation recovering exponential stability of a feedback comprising such nonlinear algebraic loop, without the need of solving it statically as long as a tuning gain is selected sufficiently high. Based on these results, in Section V we revisit the solution of [15, Remark 9] and rigorously establish its merits and limits. Finally, since both the solutions of Sections IV and V require the tuning of a high-gain parameter, we discuss in Section VI a generalized scheme where such parameter is adapted on line. Simulation results are finally discussed in Section VII.

Notation. Given two vectors u^+ and u^- in $\mathbb{R}^m$ having positive elements, for each vector $u \in \mathbb{R}^m$, the vector saturation function $\mathrm{sat}_{[u^-,u^+]}(u)$ has components $\mathrm{sat}_i(u_i) := \max(\min(u_i, {u_i}^+), -{u_i}^-)$. The deadzone function is defined as $\mathrm{dz}_{[u^-,u^+]}(u) := u - \mathrm{sat}_{[u^-,u^+]}(u)$. The subscript of sat and dz will be sometimes omitted when it is clear from the context. Given a square matrix M, $\mathrm{He}(M) := M + M^\top$, while $\Delta = \mathrm{diag}(\delta_1, \ldots, \delta_m)$ denotes a diagonal matrix having diagonal elements $\delta_1, \ldots, \delta_m$ and $\mathrm{co}\,\mathcal{S}$ denotes the (closed) convex hull of set $\mathcal{S}$.

II. Preliminaries and Problem Formulation

A. Deadzone-induced nonlinear algebraic loops

Consider the linear input-saturated plant

$$\dot{x} = Ax + B\,\mathrm{sat}_{[u^-,u^+]}(\breve{u}), \tag{1}$$

with state $x \in \mathbb{R}^n$, input $\breve{u} \in \mathbb{R}^m$ and matrices A and B of appropriate size. When dealing with the bounded stabilization problem for (1), a large number of existing works provide design techniques to optimally choose two gains K and L, of appropriate dimensions, leading to the implicit equation

$$\breve{u} = \nu + L\,\mathrm{dz}_{[u^-,u^+]}(\breve{u}), \quad \nu := Kx, \tag{2}$$

whose solution is guaranteed to exist and to enjoy desirable globally Lipschitz properties. In particular, the following definition has been introduced in [10].

Definition 1. The nonlinear algebraic loop (2) is *well-posed* if, for each selection of $\nu \in \mathbb{R}^m$, there exists a single value of $\breve{u}$ satisfying the implicit equation (2).

Remark 1. According to (2), we could only consider selections of ν in the image of matrix K; however, typically K is a large matrix, with full row rank, hence its image is the whole space.

Figure 1 shows a block diagram of the interconnection (1), (2). Based on the above definition, the results in [10] and [17] proved the following necessary and sufficient conditions.

Proposition 1. *The nonlinear algebraic loop* (2) *is well-posed if and only if* $\det(I - L\Delta) > 0$ *for all diagonal matrices* $\Delta \in \boldsymbol{\Delta}$*, where*

$$\boldsymbol{\Delta} := \{\Delta = \mathrm{diag}(\delta_1, \ldots, \delta_m) : \delta_i \in \{0, 1\}, \forall i = 1, \ldots, m\}. \tag{3}$$

Moreover, when the algebraic loop is well-posed, 1) its solution is given by a globally Lipschitz function $\breve{u} = \zeta(\nu)$ *and 2) all the matrices in the set*

$$\mathcal{S} := \{S := I - L\Delta \ : \ \Delta \in \mathrm{co}\,\boldsymbol{\Delta}\}$$

are non-singular. Finally, the existence of a matrix U *satisfying*

$$U > 0 \text{ diagonal}, \quad LU + UL^\top - 2U < 0 \tag{4}$$

is a sufficient condition for well-posedness of (2)*. According to [32, Def. 5], property* (4) *corresponds to requiring that matrix* $L - I$ *be Lyapunov Diagonally Stable.*

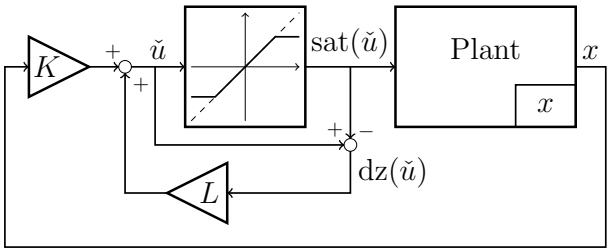

Fig. 1. Block diagram of the closed loop (1), (2) involving a nonlinear algebraic loop.

B. An LMI-based design method

An example of control design providing well-posed selections of the gains K and L in (2) is the solution of the LMIs in the next proposition, which is a classical result (see, e.g., [37], [25] but also the more recent works [22], [20] for its proof).

Proposition 2. *Given plant* (1)*, define the conservative limits vector* $\bar{u} := \min\{u^+, u^-\}$*, containing the component-wise minimum of the saturation limits* $u^+, u^- \in \mathbb{R}^m$*. If there exist*

matrices $Q = Q^\top > 0$, $U > 0$ diagonal, and W, X, Y of appropriate dimensions, satisfying

$$\mathrm{He}\begin{bmatrix} AQ + BW & -BU + BX \\ W + Y & X - U \end{bmatrix} < 0 \tag{5a}$$

$$\begin{bmatrix} \bar{u}_k^2 & Y_k \\ Y_k^\top & Q \end{bmatrix} \geq 0 \qquad k = 1 \dots m, \tag{5b}$$

where $\bar{u}_k$ indicates the k-th component of vector $\bar{u}$ and Y_k denotes the k-th row of Y, then the feedback interconnection (1), (2) *with $K = WQ^{-1}$ and $L = XU^{-1}$ is such that*

i) *the nonlinear algebraic loop* (2) *is globally well-posed and its solution is given by a globally Lipschitz function $\nu \mapsto \breve{u} = \zeta(\nu)$;*

ii) *selecting the Lyapunov function $V(x) = x^\top Q^{-1} x$, there exist $\underline{c}_V > 0$, $\bar{c}_V > 0$, and $\mu > 0$ such that*

$$\underline{c}_V \|x\|^2 \leq V(x) \leq \bar{c}_V \|x\|^2, \quad \forall x \in \mathbb{R}^n, \tag{6}$$

and, for all $x \in \mathcal{E}(V, 1) := \{x : V(x) \leq 1\}$,

$$\dot{V}(x) := \langle \nabla V(x), Ax + B \operatorname{sat}(\breve{u}) \rangle \leq -\mu \|x\|^2. \tag{7}$$

iii) *if $Y = 0$, then* (7) *holds globally.*

Remark 2. A consequence of item (ii) is that the origin is a locally exponentially stable equilibrium for the closed-loop system with basin of attraction containing the ellipsoidal estimate $\mathcal{E}(V, 1)$. Item iii) implies that the origin is globally exponentially stable. Well-posedness of the nonlinear algebraic loop follows from the sufficient condition (4), which is guaranteed by (5a) because $X = LU$. □

Remark 3. The scheme of Figure 1 may represent any output feedback controller with a linear plant and possibly also with a linear anti-windup action (e.g., of the "Direct Linear Anti-Windup" type discussed in [7, Part II]). In particular, any such dynamics may be transformed into an "Augmented Plant" whose state x comprises all the dynamical elements of such nonlinear closed loops, while matrices K and L incorporate the appropriate feedback selections (the strictly proper part in K and the algebraic part in L). One such example, shown in Figure 8, is discussed in Example 4 of Section VII. □

C. Problem statement

We aim at providing algorithmic solutions to find $\breve{u}$, given Kx in (2). To this end, we rely on introducing additional states in the loop, to address the following two goals:

1) *Static goal*: Given a constant selection of $\nu = Kx$ in (2), obtain an asymptotic estimate of the solution $\breve{u}$ of the algebraic loop;
2) *Dynamic goal*: Given a closed-loop system (1), (2) satisfying Lyapunov-induced (local or global) stability properties, provide an implementation not requiring the explicit solution ζ (of Proposition 1) while guaranteeing the same estimate of the region of attraction.

Before presenting our proposed solution, we provide some motivating examples, showing that a solution cannot be generally obtained by following an intuitive, empirical approach. In particular, with reference to the two block diagrams represented in Figure 2, we will disprove the effectiveness of the intuitive solution of transforming the algebraic relation (2) into a sequential algorithm (discrete-time approach, represented in Figure 2, left), or into a continuous-time first-order filter (continuous-time approach, represented in Figure 2, right).

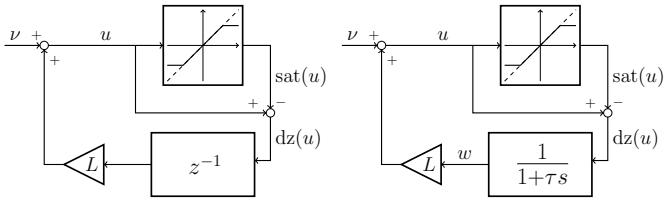

Fig. 2. Two heuristic approaches for solving the static goal of Section II-C. Their failure is discussed in Examples 1 and 2.

Example 1. (Failure of a heuristic discrete-time approach.) With reference to the left diagram of Figure 2, an intuitive approach stems from the common practice of adding a so-called "memory block" in the Simulink implementation of the feedback loop multiplying L in the block diagram of Figure 1. From the stability analysis viewpoint, this solution can be well characterized by studying the discrete-time feedback shown in Figure 2, left. Focusing on the static goal mentioned at item 1) above (which removes irrelevant complications induced by the extra dynamics of the plant), this corresponds to studying the discrete-time nonlinear system

$$u(k+1) = L \, \mathrm{dz}_{[u^-, u^+]}(u(k)) + \nu. \tag{8}$$

While $\breve{u} = \zeta(\nu)$ is certainly the unique equilibrium of dynamics (8) under our well-posedness assumption (cf. Definition 1), this does not imply attractivity of this equilibrium. Indeed, it is rather simple to construct selections of L leading to a well-posed algebraic loop, as easily checked from Proposition 1, and at the same time to non-converging solutions to (8). For example, consider the scalar examples

$$u(k+1) = -3 \, \mathrm{dz}_{[-1,1]}(u(k)) + 2, \qquad u(0) = 0, \tag{9}$$

$$u(k+1) = -2 \, \mathrm{dz}_{[-1,1]}(u(k)) + 5, \qquad u(0) = 0, \tag{10}$$

and note that with u being a scalar, the exact solution of the algebraic loop can be determined by the following equation, [1] issued from [20, Lemma 3],

$$\breve{u} = \zeta(\nu) = \nu + L(I - L)^{-1} \, \mathrm{dz}_{[-1,1]}(\nu), \tag{11}$$

which provides $\breve{u} = 5/4$ and $\breve{u} = 7/3$, respectively, corresponding to the horizontal dashed lines in the two plots of Figure 3. The two (unique) solutions to the initial value problems (9) and (10) are also shown by the black dots at the left and right of Figure 3, respectively. From these traces it appears that (9) generates a non-converging and non-diverging evolution, while (10) generates an exponentially diverging solution, thereby showing the failure of the heuristic approach at the left of Figure 2. ⋆

Example 2. (Failure of a continuous-time approach.) A viable approach was suggested in [15, Remark 9], where the

[1] The explicit expression (11) for ζ is only valid for the special case $m = 1$, as proven in [20, Lemma 3].

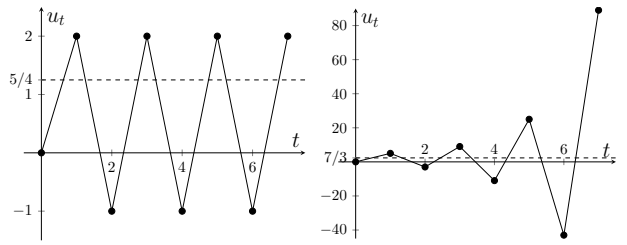

Fig. 3. Solutions of the discrete-time systems in (9), left, and (10), right, stemming from the heuristic solution shown at the left of Figure 2.

conservative well-posedness condition (4) was assumed. The idea is to add a first order filter with transfer function $\frac{1}{1+\tau s}$ in the feedback loop multiplying L in the block diagram of Figure 1, as shown at the right of Figure 2. Without giving a proof, [15, Remark 9] conjectured that there exists a small enough value of the time constant $\tau > 0$ (a sufficiently fast filter) that provides a converging solution to the problem. In this paper (see Section V) we show that this conjecture is true when condition (4) holds, but the solution is not effective for general well-posed algebraic loops. In fact, the dynamics associated with this solution corresponds to the following linear continuous-time differential equation:

$$\dot{w} = \frac{1}{\tau}\Big(\mathrm{dz}_{[u^-,u^+]}(Lw+\nu) - w\Big), \tag{12}$$

where τ should be sufficiently small. To show this is not a viable approach for general well-posed loops, we rewrite the dynamics as follows:

$$\begin{aligned}\tau\dot{w} &= -w + Lw + \nu - \mathrm{sat}_{[u^-,u^+]}(Lw+\nu)\\ &= (L-I)w - \mathrm{sat}_{[u^-,u^+]}(Lw+\nu) + \nu,\end{aligned}$$

and notice that matrix $(L - I)$ is not guaranteed to be Hurwitz. In particular, since sat is bounded, if $(L-I)$ has an exponentially unstable eigenvalue, then the results in [1] imply that there are large enough initial conditions for w leading to exponentially diverging solutions, and the exponential rate becomes increasingly fast as τ becomes increasingly small. A choice of L that satisfies both this defective condition and the necessary and sufficient well-posedness conditions of Proposition 1 cannot be found for the scalar case $m = 1$, but can be found e.g. for the case $m = 3$: the selection $L = \left[\begin{smallmatrix} 0 & 3 & 0 \\ 0 & 0 & 3 \\ -3 & 0 & 0 \end{smallmatrix}\right]$ yields exponentially unstable eigenvalues of $L - I$, while satisfying the well-posedness conditions. This counterexample shows that, in general, the right scheme of Figure 2 is not a viable solution to the static goal.

It is quite interesting that the sufficient condition (4) implies that matrix $L - I$ be Hurwitz (as certified by the diagonal positive definite matrix U). Since (4) was required in [15, Remark 9], this counterexample does not contradict that statement, which is indeed true, as proven in Section V. ⋆

Remark 4. Conditions for the convergence of the heuristic solutions could be incorporated in the design of L through appropriate robust stability conditions, e.g. enforced through LMIs coupled with system (8) or (12). However, this would introduce in the design of L additional restrictions, which we show are not necessary.

Motivated by the fact that simple intuitive approaches are not successful in general, we propose in the next section a nonlinear dynamic augmentation solving both the static and dynamic problems presented above.

III. Solution to the Static Problem

A. Proposed solution and main result

In this section we address the static goal presented at item 1) of Section II-C. In particular, we disregard the plant dynamics (1) and address the simpler (yet relevant) problem of providing a dynamic algorithm to asymptotically determine the solution $\breve{u} := \zeta(\nu)$ of the algebraic loop

$$u = L\,\mathrm{dz}_{[u^-,u^+]}(u) + \nu, \tag{13}$$

for each constant selection of $\nu \in \mathbb{R}^m$.

The approach that we propose provides global guarantees under the (non-restrictive) assumption that the algebraic loop is well-posed, as per Definition 1. Given a constant tunable gain $\bar{\alpha} > 0$ governing the speed of convergence, and inspired by [31], our solution relies on the *out-of-balance vector*:

$$y = -u + L\,\mathrm{dz}_{[u^-,u^+]}(u) + \nu. \tag{14a}$$

Based on y, we propose the following dynamic augmentation through the new state variable u:

$$\dot{u} = \bar{\alpha}\,\mathrm{dz}^*(y) := \bar{\alpha}(y - D_y\,\mathrm{sat}_{[0,|L^\top y|_{\mathrm{cw}}]}(D_y y)), \tag{14b}$$

where dz^* is defined on $\mathbb{R}^m$, while

$$D_y := \mathrm{diag}(\mathrm{sign}(L^\top y)), \tag{14c}$$

and $|\cdot|_{\mathrm{cw}}$ denotes the vector containing the component-wise absolute values of its argument. We emphasize that the right-hand side of (14b) is continuous on $\mathbb{R}^m$, because it returns zero whenever the sign in expression (14c) is evaluated at zero.

The following lemma establishes desirable properties of the right-hand side of (14b). Its proof is deferred to the end of Section III-B.

Lemma 1. *Function* dz^* *in* (14b) *is globally Lipschitz and independent of the conventional value chosen for* $\mathrm{sign}(0)$. *Moreover, function* dz^* *lies in the sector* $[0, 1]$ *and if the algebraic loop* (13) *is well-posed, then* $\mathrm{dz}^*(y) = 0$ *if and only if* $y = 0$.

Theorem 1. *Let the algebraic loop* (13) *be well-posed. For any constant gain* $\bar{\alpha} > 0$ *and each constant input* $\nu \in \mathbb{R}^m$, *the interconnection* (14) *has a globally exponentially stable equilibrium point* $u = \breve{u} = \zeta(\nu)$ *with exponential decay rate proportional to* $\bar{\alpha}$.

While we postpone the proof of Theorem 1 to Section III-C, we provide in the next section a deeper insight about its game-theoretic motivation.

B. Game-theoretic motivation of the proposed solution

We provide here the essential intuition behind selection (14) together with a suitable interpretation in terms of game theory. To this end, first observe that, from well-posedness,

Proposition 1 establishes that matrix $I - L\Delta$ is non-singular for all $\Delta \in \mathbf{\Delta}$, as defined in (3).

Then, inspired by [31], it makes sense to introduce the out-of-balance vector y in (14a) and select a suitable dynamics $\dot{u} = v$, where the selection of v, a design degree of freedom, is carried out by inspecting the time derivative of the Lyapunov-like function $W(y) := \frac{1}{2} y^\top y$. The remaining derivations stem from the approach of [31], with the caveat that $u \mapsto W(y(u))$ is not a smooth function, hence we need to pay special attention to the fact that there are points in the state space where $\dot{W}$ is not defined. To deal with this issue, we exploit results from Lipschitz Lyapunov functions, given in [38, §4.5]. In particular, denoting by $\dfrac{\partial y}{\partial u} \in \mathbb{R}^{m \times m}$ the Jacobian of y with respect to u, and using the fact that, by Rademacher's theorem, the globally Lipschitz saturation function is differentiable almost everywhere, we may write for almost all $u \in \mathbb{R}^m$,

$$\dot{W} = y^\top \dot{y} = y^\top \frac{\partial y}{\partial u} \dot{u} = -y^\top (I - L\Delta_u)\, v, \tag{15}$$

where $\Delta_u \in \mathbf{\Delta}$ represents the Jacobian of the *deadzone* function $\mathrm{dz}_{[u^-,u^+]}$, wherever it is differentiable. This matrix is well defined almost everywhere and has diagonal terms either equal to 1 or 0, therefore it belongs to the set $\mathbf{\Delta}$ in (3).

In an interpretation coming from game theory, in particular coming from min-max games, it is possible to interpret the time derivative of W in (15) as if it were governed by two players. The first player, the *minimizer*, decides Δ_u so as to minimize $-\dot{W}$, while the second player, the *maximizer*, decides $\dot{u} = v$ in order to maximize $-\dot{W}$ and then get exponential stability. While the Jacobian matrix Δ_u depends on the state u, since we associate the choice of Δ_u with a clever "nasty" minimizer, we allow Δ to take any value in the set $\mathbf{\Delta}$ of (almost) all possible values of the gradient. Actually, even more so, since we would like to exploit useful properties of convex (and compact) sets, rather than allowing Δ to take values in the non-convex set $\mathbf{\Delta}$, we expand the allowable selections to its convex hull $\operatorname{co} \mathbf{\Delta}$, which is also compact by definition. Summarizing, we perform the selection of v in (15) with the aim of finding the saddle point of the game $\gamma^+ = \gamma^-$ where, from (15),

$$\gamma^-(y) = \min_{\Delta \in \operatorname{co}\mathbf{\Delta}} \max_{\|v\| \le \alpha(y)\|y\|} y^\top (I - L\Delta)\, v \tag{16a}$$

$$\gamma^+(y) = \max_{\|v\| \le \alpha(y)\|y\|} \min_{\Delta \in \operatorname{co}\mathbf{\Delta}} y^\top (I - L\Delta)\, v, \tag{16b}$$

and where we restricted v to the compact convex set $\|v\| \le \alpha(y)\|y\|$, for an arbitrary positive scalar $\alpha(y)$, to ensure suitable regularity of the min-max problem.

Since the cost function in (16) is linear in the two decision variables Δ and v, which belong to convex and compact sets, then $\gamma^+ = \gamma^-$ (see [39, §7.13, Thm 1]). In particular, the maximizer will always choose the maximal v in the direction of $(I - L\Delta^\star)y$, where $\Delta^\star$ is the choice of the minimizer. As a consequence, the resulting cost is necessarily non-negative and the minimizer will aim at reducing its norm:

$$\left(\min_{\Delta \in \operatorname{co}\mathbf{\Delta}} \| \left(I - \Delta L^\top\right) y \| \right)^2 = \min_{0 \le \delta_i \le 1} \sum_{i=1}^{m} (y_i - \delta_i\, L_i^\top y)^2, \tag{17}$$

where L_i denotes the ith column of matrix L. Since each diagonal element δ_i of Δ only appears in one of the scalars in the sum at the right hand side, we can determine the following selection of the diagonal elements $\delta_i^\star$ of $\Delta^\star$:

$$\delta_i^\star = \operatorname{sat}_{[0,1]}\left(\frac{y_i}{L_i^\top y}\right) \qquad \text{if } L_i^\top y \neq 0,$$

$$\delta_i^\star = 0 = \operatorname{sat}_{[0,0]}(y_i) = \operatorname{sat}_{[0, L_i^\top y]}(y_i), \qquad \text{if } L_i^\top y = 0.$$

After some straightforward derivations, we may combine the two previous conditions in the following unified expression:

$$\delta_i^\star L_i^\top y = \operatorname{sign}(L_i^\top y) \operatorname{sat}_{[0, |L_i^\top y|]}\left(\operatorname{sign}(L_i^\top y) y_i\right), \tag{18}$$

which can be written in vector form as

$$\Delta^\star L^\top y = D_y \operatorname{sat}_{[0, |L^\top y|_{\mathrm{cw}}]}\left(D_y y\right),$$

where $|\cdot|_{\mathrm{cw}}$ denotes the vector containing the component-wise absolute values of its argument and D_y is defined in (14c). Finally, we may provide the complete expression of the minimized vector in (17) as

$$\left(I - \Delta^\star L^\top\right) y = y - D_y \operatorname{sat}_{[0, |L^\top y|_{\mathrm{cw}}]}\left(D_y y\right), \tag{19}$$

which coincides with the vector $\mathrm{dz}^*(y)$ defined in (14b).

Note that the derivations above are independent of the choice of function $y \mapsto \alpha(y)$ appearing in (16). In particular, selecting $\alpha(0) = 1$ and, for $y \neq 0$, [2]

$$\alpha(y) = \bar{\alpha} \frac{\| y - D_y \operatorname{sat}_{[0, |L^\top y|_{\mathrm{cw}}]}\left(D_y y\right) \|}{\|y\|} = \bar{\alpha} \frac{\| \mathrm{dz}^*(y) \|}{\|y\|} > 0, \tag{20}$$

we obtain exactly the solution $v = \bar{\alpha}\, \mathrm{dz}^*(y)$ as in (14b).

Based on the derivations above, we are now ready to prove Lemma 1.

Proof of Lemma 1. Let us first notice that expression (19) and the properties of well-posed algebraic loops, established in Lemma 1, imply that matrix $I - \Delta^\star L^\top$ is invertible, so for each $y \neq 0$ we have $\mathrm{dz}^\star(y) = (I - \Delta^\star L^\top) y \neq 0$.

For the rest of the proof, due to the expression of dz^* in (14b), it is enough to show that $D_y \operatorname{sat}_{[0, |L^\top y|_{\mathrm{cw}}]}\left(D_y y\right)$ is globally Lipschitz, independent of the value $\operatorname{sign}(0)$ and lies in the sector $[0, 1]$. From (18) this function is decentralized, so we can focus on each component $i \in \{1, \dots, m\}$ in (18). First of all, notice that when $L_i^\top y = 0$, the function is zero (because $\operatorname{sat}_{[0,0]} \equiv 0$), regardless of the value of $\operatorname{sign}(L_i^\top y) = \operatorname{sign}(0)$. Moreover, the function is globally Lipschitz and belongs to the sector $[0, 1]$, due to the corresponding properties of the saturation function, and the fact that the saturation limit $L_i^\top y$ depends linearly on y. ■

C. Proof of Theorem 1

For the proof of Theorem 1 we will use the next lemma, which is a corollary of [39, §3.12, Thm 1].

[2] Positivity of $\alpha(y)$ in (20) when $y \neq 0$ follows from the left expression in (19) and the fact that, from Proposition 1, all the matrices in $\mathcal{S}$ are non-singular.

Lemma 2. *Given a closed and convex set $\mathcal{Z}$ of $\mathbb{R}^m$, the unique solution $z^\star$ of the minimization problem $\min_{z\in\mathcal{Z}} \|z\|^2$, satisfies ${z^\star}^\top z \geq {z^\star}^\top z^\star$, for all $z \in \mathcal{Z}$.*

Proof. The result follows from [39, §3.12, Thm 1] applied with the following selections: $H = \mathbb{R}^m$, $K = \mathcal{Z}$, $x = 0$, $k_0 = z^\star$, $k = z$. ∎

In addition, for the proof of the theorem, we will exploit the continuity of function dz^* and apply the following non-smooth Lyapunov result, which is an immediate consequence of the discussion in [40, page 99], or the recent result in [41, Prop. 1] combined with [38, §4.5].

Proposition 3. *Consider an autonomous system $\dot\xi = f(\xi)$ with $f : \mathbb{R}^n \to \mathbb{R}^n$ continuous, a compact set $\mathcal{A}$ and an open set $\mathcal{D}$ such that $\mathcal{A} \subset \mathcal{D} \subset \mathbb{R}^n$. Assume that there exists a locally Lipschitz function $\mathcal{V} : \mathcal{D} \to \mathbb{R}$ such that*

$$c_1\|\xi\|_{\mathcal{A}}^2 \leq \mathcal{V}(\xi) \leq c_2\|\xi\|_{\mathcal{A}}^2, \quad \forall\, \xi \in \mathcal{D} \tag{21}$$

$$\langle \nabla\mathcal{V}(\xi), f(\xi)\rangle \leq -2c_3\mathcal{V}, \text{ for almost all } \xi \in \mathcal{D}, \tag{22}$$

where $\|\xi\|_{\mathcal{A}} = \min_{x\in\mathcal{A}} \|\xi - x\|$ denotes the point-to-set distance. Then $\mathcal{A}$ is locally exponentially stable with exponential rate c_3 and with basin of attraction containing any sublevel set of $\mathcal{V}$ contained in $\mathcal{D}$. In particular, if $\mathcal{D} = \mathbb{R}^n$, then $\mathcal{A}$ is globally exponentially stable.

Proof: Under the stated assumptions, due to continuity of the dynamics, even if (22) holds almost everywhere, we may follow the derivations of the 8 steps reported in [40, page 99-100], relying on Clarke's generalized directional derivative, to obtain an exponential bound on $t \mapsto \mathcal{V}(\xi(t))$, with decay rate $2c_3$, for any solution of $\dot\xi = f(\xi)$. Then, using (21), we may transform this bound in a uniform global exponential bound for $t \mapsto \|\xi(t)\|_{\mathcal{A}}$, with decay rate c_3. ∎

Proof of Theorem 1. This proof is inspired by the techniques in [31] and the ensuing derivations of the previous section, combined with the non-smooth result of Proposition 3. First note that the dynamics of system (14) is autonomous once $\bar\alpha$ and ν have been fixed. Consider then the Lyapunov-like function $W(y) := \frac{1}{2}y^\top y$, discussed in Section III-B. Denoting by ζ the globally Lipschitz (with Lipschitz constant ℓ_ζ) solution of (2) established in Proposition 1, we have from (14a) that $\check u = \zeta(\nu)$, and $u = \zeta(\nu - y)$, which imply

$$\|u - \check u\| = \|\zeta(\nu - y) - \zeta(\nu)\| \leq \ell_\zeta\|y\|. \tag{23}$$

Moreover, exploiting $\nu = \check u - L\,\mathrm{dz}_{[u^-,u^+]}(\check u)$, from (13), and using the Lipschitz property of the deadzone nonlinearity, we also get from (14a),

$$\begin{aligned}\|y\| &= \|\check u - L\,\mathrm{dz}_{[u^-,u^+]}(\check u) - u + L\,\mathrm{dz}_{[u^-,u^+]}(u)\| \\ &\leq \|\check u - u\| + \|L\,\mathrm{dz}_{[u^-,u^+]}(\check u) - L\,\mathrm{dz}_{[u^-,u^+]}(u)\| \\ &\leq (1 + \|L\|)\|u - \check u\|. \end{aligned}\tag{24}$$

Combining bounds (23) and (24), we obtain

$$c_{1W}\|u - \check u\|^2 \leq 2W(y) \leq c_{2W}\|u - \check u\|^2, \tag{25}$$

where $c_{1W} := \ell_\zeta^{-2}$ and $c_{2W} := (1 + \|L\|)^2$.

To establish an upper bound on $\dot W$, consider expression (15) and notice that, with $\dot u = v$ selected as in (14) and enforcing the equality in (19), it leads to

$$\dot W = y^\top\dot y = -\bar\alpha z^\top z^\star, \text{ for almost all } y, \tag{26}$$

where, using the notation of Lemma 2, we defined

$$\begin{aligned}\mathcal{Z} &= \Big\{ \big(\Delta L^\top - I\big)\, y \,\big|\, \Delta \in \mathrm{co}(\boldsymbol{\Delta})\Big\}, \\ z &= \big(\Delta_u L^\top - I\big)\, y, \quad z^\star = \big(\Delta^\star L^\top - I\big)\, y.\end{aligned}$$

As proven in the previous subsection, in the discussion between equations (17) and (19), $\Delta^\star$ is a minimizer of (17) over $\mathrm{co}(\boldsymbol{\Delta})$. This implies that $z^\star$ is the (unique, by Lemma 2) minimizer of $\|z\|$ over $\mathcal{Z}$. [3] Recalling the fact that $\Delta_u \in \boldsymbol{\Delta}$ and that $\boldsymbol{\Delta} \subset \mathrm{co}(\boldsymbol{\Delta})$, we have that $z \in \mathcal{Z}$ and applying Lemma 2, we get $-{z^\star}^\top z \leq -{z^\star}^\top z^\star$, which provides the following negative upper bound for (26):

$$\dot W \leq -\bar\alpha z^\top z^\star \leq -\bar\alpha\|z^\star\|^2, \text{ for almost all } y. \tag{27}$$

As a final step of the proof, from item 2) of Proposition 1, we have that $y^\top(-I + L\Delta) \neq 0$ for all $\Delta \in \mathrm{co}(\boldsymbol{\Delta})$ and all $y \neq 0$. Therefore the following minimum exists and is positive:

$$\begin{aligned}\inf_{\|y\|\neq 0} \frac{\|z^\star\|}{\|y\|} &= \inf_{\substack{\Delta\in\mathrm{co}(\boldsymbol{\Delta})\\ \|y\|\neq 0}} \frac{\|y^\top\left(-I + L\Delta^\star\right)\|}{\|y\|} \\ &= \min_{\|y\|=1} \|y^\top\left(-I + L\Delta^\star\right)\| = \beta > 0,\end{aligned}$$

which can be replaced in (27) to get

$$\dot W \leq -\bar\alpha\frac{\|z^\star\|^2}{\|y\|^2}\|y\|^2 \leq -\bar\alpha\beta^2\|y\|^2 = -2\bar\alpha\beta^2 W(y), \tag{28}$$

which holds for almost all y. Even though bound (28) holds almost everywhere, also using bounds (25), we may apply Proposition 3 with $\mathcal{A} = \{\check u\}$ to obtain a uniform global exponential bound on $u - \check u$, with decay rate given by $\bar\alpha\beta^2 > 0$ for any solution of (14). ∎

Example 3. We provide simulation results for the 3-input counterexample, with $L = \left[\begin{smallmatrix} 0 & 3 & 0 \\ 0 & 0 & 3 \\ -3 & 0 & 0 \end{smallmatrix}\right]$, constructed in Example 2 to illustrate the generic unsuitability of the linear solution proposed in [15, Remark 9], in cases where the conservative condition (4) does not hold. To see that this selection of L does not satisfy (4), note that (4) would imply that $L - I$ be a Hurwitz matrix, whereas $L - I$ has exponentially unstable modes for this selection. In this example we fix the saturation bounds at $u^+ = u^- = 1$ for all three inputs.

Figure 4 shows the exponentially converging responses (solid lines) obtained from the nonlinear solution (14) compared with the exponentially diverging responses (dashed lines) obtained from the linear solution (12), thus confirming the results in Example 2 and Theorem 1. Figure 5 also confirms the result of Theorem 1 in terms of speed of convergence, which is clearly accelerated as $\bar\alpha$ is increased in the nonlinear solution (14). ⋆

[3] We emphasize the interesting fact that the minimizer $\Delta^\star$ is not unique, whereas convexity of $\mathcal{Z}$ implies that the minimizer $z^\star$ is instead unique, and clearly coincides with the expression in (19).

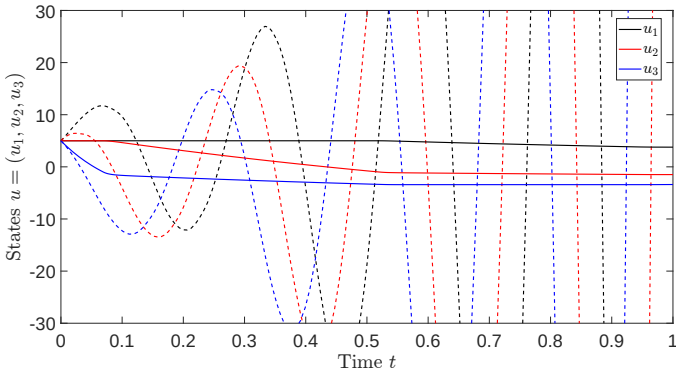

Fig. 4. Evolution of u for Example 3. Dashed lines: exponentially diverging evolution of u for the linear solution (12). Solid lines: evolution of u for the nonlinear solution (14) with $\bar{\alpha} = 10$, converging exponentially to the solution of the nonlinear algebraic loop (2).

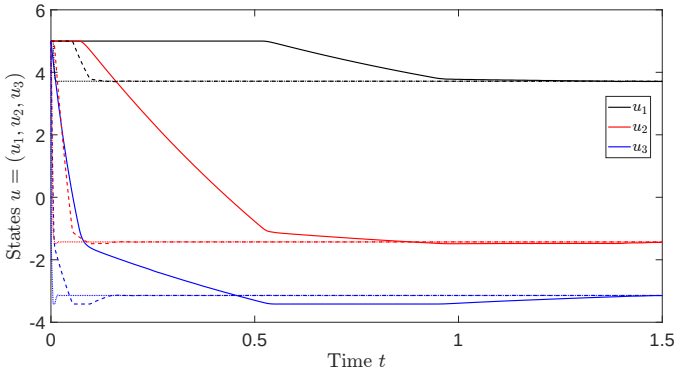

Fig. 5. Example 3: evolution of u for the nonlinear solution (14) for increasing selections of $\bar{\alpha} = 10$ (solid lines), $\bar{\alpha} = 100$ (dashed lines), $\bar{\alpha} = 1000$ (dotted lines).

IV. Solution to the Dynamical Problem

Let us now address the global and local formulations of the problem at item 2 in Section II-C. In particular, let us assume that a stabilizer as in (2) has been designed for a plant as in (1), which ensures well-posedness of the algebraic loop and the existence of a Lyapunov function V satisfying (6) and (7) for some scalar $\mu > 0$, either globally or in the ellipsoidal sublevel set $\mathcal{E}(V,1) = \{x \in \mathbb{R}^n : V(x) \leq 1\}$.

By combining the approach of Section III with the original interconnection, we propose the following dynamically augmented implementation

$$\begin{aligned} \dot{x} &= Ax + B\,\mathrm{sat}(Kx + w), \\ \dot{w} &= \bar{\alpha}\,\mathrm{dz}^*(y) \\ y &= L\,\mathrm{dz}_{[u^-,u^+]}(u) - w, \end{aligned} \tag{29}$$

where $u = w + Kx$ and function dz^* has been defined in (14b). Since $w = u - \nu = u - Kx$, then vector y in (29) coincides with the out-of-balance vector y in (14a), namely

$$y = -u + L\,\mathrm{dz}_{[u^-,u^+]}(u) + Kx. \tag{30}$$

For this dynamically augmented feedback stabilization scheme, which is represented in Figure 6, we establish the following main result.

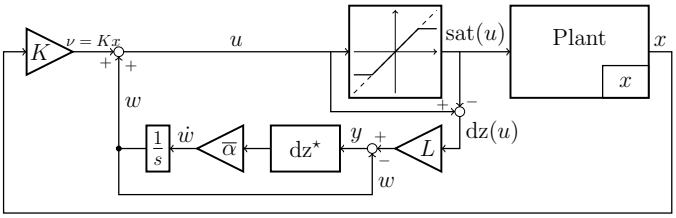

Fig. 6. Block diagram of the overall system (29).

Theorem 2. *Suppose that the algebraic loop* (2) *is well-posed and there exist a Lyapunov function V and a scalar $c_v > 0$, such that $\|\nabla V(x)\| \leq c_v \|x\|$, satisfying* (6), (7) *for all $x \in \mathcal{E}(V,1)$ (respectively, globally), for the closed loop* (1), (2).

Then there exists $\alpha^* > 0$ such that, for any $\bar{\alpha} \geq \alpha^*$, the origin of the dynamically augmented implementation (29) *is* locally exponentially stable *with basin of attraction containing the set*

$$\bar{\mathcal{E}} := \{(x,w) \in \mathbb{R}^n \times \mathbb{R}^m : x \in \mathcal{E}(V,1), w = \zeta(Kx) - Kx\}, \tag{31}$$

(respectively, globally exponentially stable*).*

While for the global case Theorem 2 shows that global exponential stability properties are fully preserved by our augmentation in (29), the local case needs more care. Indeed, since we do not assume any property of $\dot{V}(x)$ outside the sublevel set $\mathcal{E}(V,1)$, we can only recover convergence for any $x \in \mathcal{E}(V,1)$ as long as the initialization of w ensures $y = 0$ (namely $w = \zeta(Kx) - Kx$). This is the motivation for the guarantees of Theorem 2 about $\bar{\mathcal{E}}$. Alternative initializations of w are also allowed but should be compensated by a smaller amplitude of $V(x)$. A quantitative margin can be extracted by the composite Lyapunov-like function

$$U(x,y) := V(x) + W(y) = V(x) + \frac{1}{2}\|y\|^2 \tag{32}$$

that we use in the proof below. Indeed, the set where $U(x,y) \leq 1$ is contained in the basin of attraction. Note that through the continuous dependence $y = L\,\mathrm{dz}_{[u^-,u^+]}(Kx + w) - w$ in (29), $U(x,y)$ is actually a function of the state (x,w).

Proof of Theorem 2 Using (6), we obtain for function U in (32)

$$\underline{c}_U \left\|\left[\begin{smallmatrix} x \\ y \end{smallmatrix}\right]\right\|^2 \leq U(x,y) \leq \bar{c}_U \left\|\left[\begin{smallmatrix} x \\ y \end{smallmatrix}\right]\right\|^2, \tag{33}$$

where $\underline{c}_U = \min\{\frac{1}{2}, \underline{c}_V\}$ and $\bar{c}_U = \max\{\frac{1}{2}, \bar{c}_V\}$.

To the end of computing $\dot{U}$ along dynamics (29), we study the two terms separately. For $\dot{V}$, from the global Lipschitz property of the saturation function combined with (23), we establish the bound:

$$\|\mathrm{sat}(u) - \mathrm{sat}(\check{u})\| \leq \|u - \check{u}\| \leq \ell_\zeta \|y\|. \tag{34}$$

Then, exploiting (7), we obtain that for all $x \in \mathcal{E}(V,1)$ (respectively, for all $x \in \mathbb{R}^n$),

$$\begin{aligned} \dot{V}(x) &= \langle \nabla V(x), Ax + B(\mathrm{sat}(u) + \mathrm{sat}(\check{u}) - \mathrm{sat}(\check{u})) \rangle \\ &\leq -\mu\|x\|^2 + \|\nabla V(x)\|\|B\|\|\,\mathrm{sat}(u) - \mathrm{sat}(\check{u})\| \\ &\leq -\mu\|x\|^2 + c_v \ell_\zeta \|x\|\|B\|\|y\|. \end{aligned} \tag{35}$$

To characterize $\dot{W}$, note that the global Lipschitz property of the saturation and of the solution ζ of the algebraic loop implies that

$$\|Ax + B\,\mathrm{sat}(\check{u})\| \leq \|A\|\|x\| + \|B\|\|\zeta(Kx)\| \leq \theta\|x\|, \quad (36)$$

with $\theta := \|A\| + \ell_\zeta\|B\|\|K\|$. Moreover, since $u = w + Kx$, then (29) provides

$$\dot{u} = \bar{\alpha}\,\mathrm{dz}^*(y) + K\dot{x}.$$

Using again (34), the expression for y in (30), and the upper bound in (28), for almost all y, we get

$$\begin{aligned}\dot{W}(y) &= y^\top\dot{y} = y^\top\left(\frac{\partial y}{\partial u}\dot{u} + \frac{\partial y}{\partial x}\dot{x}\right) \quad (37)\\ &= y^\top(-I + L\Delta_u)(\bar{\alpha}\,\mathrm{dz}^*(y) + K\dot{x}) + y^\top K\dot{x}\\ &\leq -2\bar{\alpha}\beta^2 W(y) + y^\top L\Delta_u K(Ax + B\,\mathrm{sat}(\check{u})) +\\ &\qquad + y^\top L\Delta_u KB(\mathrm{sat}(u) - \mathrm{sat}(\check{u}))\\ &\leq -\bar{\alpha}\beta^2\|y\|^2 + \theta\|y\|\|L\|\|K\|\|x\| +\\ &\qquad + \ell_\zeta\|y\|\|L\|\|KB\|\|y\|,\end{aligned}$$

where we used the fact that $\|L\Delta_u\| \leq \|L\|$ for all $u \in \mathbb{R}^m$. Combining the bounds in (35) and (37), for almost all $(x, y) \in \mathcal{E}(V, 1) \times \mathbb{R}^m$ (respectively, for almost all $(x, y) \in \mathbb{R}^n \times \mathbb{R}^m$), we get

$$\dot{U}(x,y) \leq \begin{bmatrix}\|x\|\\ \|y\|\end{bmatrix}^\top \begin{bmatrix}-\mu & \frac{1}{2}(c_v\ell_\zeta\|B\| + \theta\|L\|\|K\|)\\ * & -\bar{\alpha}\beta^2 + \ell_\zeta\|L\|\|KB\|\end{bmatrix}\begin{bmatrix}\|x\|\\ \|y\|\end{bmatrix}, \quad (38)$$

where "*" denotes symmetric elements. Then, for all

$$\bar{\alpha} > \alpha^\star := \frac{\mu\ell_\zeta\|L\|\|KB\| + \frac{1}{4}(c_v\ell_\zeta\|B\| + \theta\|L\|\|K\|)^2}{\mu\beta^2}, \quad (39)$$

the matrix in the quadratic form in (38) is negative definite. This implies, for a small enough positive scalar ϵ and for any such $\bar{\alpha}$,

$$\dot{U}(x,y) \leq -\epsilon\,\|[\begin{smallmatrix}x\\ y\end{smallmatrix}]\|^2 \leq -\frac{\epsilon}{\bar{c}_U}U(x,y), \text{ for a. all } (x,y) \in \mathcal{D}, \quad (40)$$

where we used the second inequality in (33) and where $\mathcal{D} := \mathcal{E}(V, 1) \times \mathbb{R}^m$ (respectively, $\mathcal{D} := \mathbb{R}^n \times \mathbb{R}^m$).

Considering the last expression in (29) yields

$$\|y\| \leq (1 + \|L\|)\|u\| + \|K\|\|x\|. \quad (41)$$

Moreover, rearranging (30) and using the global Lipschitz property of ζ, we get

$$\|u\| \leq \|\zeta(Kx - y)\| \leq \ell_\zeta\|K\|\|x\| + \ell_\zeta\|y\|,$$

which then gives

$$\|w\| = \|u - Kx\| \leq (1 + \ell_\zeta)\|K\|\|x\| + \ell_\zeta\|y\|. \quad (42)$$

Combining (41) and (42) with (33), we prove that there exist scalars $c_{1U} > 0$ and $c_{2U} > 0$ satisfying

$$c_{1U}\,\|[\begin{smallmatrix}x\\ w\end{smallmatrix}]\|^2 \leq U(x,y) \leq c_{2U}\,\|[\begin{smallmatrix}x\\ w\end{smallmatrix}]\|^2. \quad (43)$$

To complete the proof, we fist notice that U can be seen as a function of the state $\xi = (x, w)$ as follows

$$\mathcal{V}(x,w) := U(x, L\,\mathrm{dz}_{[u^-,u^+]}(Kx + w) - w), \quad (44)$$

and then (40) and (43) establish (22) and (21), respectively. As a consequence, applying Proposition 3 with $\mathcal{V}$ in (44) and $\mathcal{A} = \{(x, w) : x = 0, w = 0\}$, we establish exponential stability of $\mathcal{A}$ (the origin).

While for the global case it is evident that the result is global because $\mathcal{D} := \mathbb{R}^n \times \mathbb{R}^m$ covers the whole space, for the local case, according to Proposition 3, an estimate of the basin of attraction is given by

$$\mathcal{E}(\mathcal{V}, 1) := \{(x, w) \in \mathbb{R}^n \times \mathbb{R}^m :\ \mathcal{V}(x, w) \leq 1\}.$$

In particular, since $y = 0$ if and only if $u = \zeta(Kx)$, or equivalently $w + Kx = \zeta(Kx)$, then for any $(x, w) \in \bar{\mathcal{E}}$, as defined in (31), we have $\mathcal{V}(x, w) = U(x, y) = V(x) \leq 1$, which implies $(x, w) \in \mathcal{E}(\mathcal{V}, 1)$, thus completing the proof. ■

Remark 5. As $\bar{\alpha} \to +\infty$, the two eigenvalues of the matrix in (38) tend respectively to $-\infty$ and $-\mu$. Therefore an upper bound on the convergence rate to the origin is represented by the rate μ of the feedback involving the exact solution of the algebraic loop. However, with smaller values of $\bar{\alpha} \geq \alpha^*$, the largest eigenvalue of the matrix in (38) gets larger than $-\mu$, thus we can only guarantee a slower convergence rate, while still ensuring (global) exponential stability of the origin. □

Remark 6. In the existing literature (see, e.g., [15], [37], [25]), algebraic loops of the type (2) are often encountered in conjunction with quadratic performance guarantees in terms of the $\mathcal{L}_2$ gain from an exogenous signal d entering linearly in the closed-loop dynamics to a linear performance output $z = C_z x + D_{zu}\,\mathrm{sat}(u) + D_{zd}d$. The typical scenario is that the quadratic decrease (7) is augmented into the disturbance attenuation bound

$$\dot{V}(x) + \frac{1}{\gamma}\|\check{z}\|^2 - \gamma\|d\|^2 \leq -\mu\|x\|^2,$$

where $\dot{V}(x) = \langle\nabla V(x), Ax + B\,\mathrm{sat}(\check{u})\rangle$ and $\check{z} := C_z x + D_{zu}\,\mathrm{sat}(\check{u}) + D_{zd}d$ corresponds to the performance output that one would obtain if implementing exactly the solution $\check{u} = \zeta(Kx)$ of the algebraic loop. Also in this case, the proof technique of Theorem 2 applies and can be followed to obtain the existence of a large enough α^* such that, for any $\bar{\alpha} > \alpha^*$, the following quadratic performance condition is satisfied:

$$\dot{U}(x,y) + \frac{1}{\gamma}\|z\|^2 - \gamma\|d\|^2 \leq -\epsilon\|\,[\begin{smallmatrix}x\\ y\end{smallmatrix}]\,\|^2, \quad (45)$$

where ϵ is constructed as in (40). Inequality (45) shows that, for a large enough $\bar{\alpha}$, the original quadratic performance can be fully recovered also when solving dynamically the nonlinear algebraic loop. The detailed calculations, which essentially exploit inequality (34), are not given here to avoid overloading the notation. □

V. Linear Solution of [15, Remark 9]

We revisit in this section the approach already summarized in Example 2, reinterpreting it as a linear counterpart of our solution presented in Sections III and IV, which successfully solves the problems in the case where the (conservative) sufficient condition (4) is satisfied, namely matrix $L-I$ is Lyapunov Diagonally Stable. This result was already suggested in [15, Remark 9] without making any precise statements. Here, exploiting the stability proof in [32, Thm 4], we prove rigorously the properties of the corresponding solution. To simplify the discussion and make suitable comparisons with the nonlinear approach of Sections III and IV, we write the linear solution (12) in terms of a scalar gain $\bar{\alpha} = \tau^{-1}$.

Let us first consider the static case where ν is constant. To the end of computing $\breve{u} = \zeta(\nu)$, consider the following selection, which can be seen as a linear counterpart of (14), and which coincides with (12) when ν is constant:

$$\dot{u} = \bar{\alpha} y = \bar{\alpha}(-u + L\,\mathrm{dz}_{[u^-,u^+]}(u) + \nu), \tag{46}$$

where $\bar{\alpha}$ is a constant gain and y is the out-of-balance vector introduced in (14a).

We already established in Example 2 (see also Example 3) that there are cases where the algebraic loop is well-posed but the dynamical system (46) has an unstable equilibrium. However, we show below that when the (conservative) sufficient condition (4) is satisfied (this was the case in [15, Remark 9]), then (46) is an effective solution to our static problem.

Theorem 3. *Assume that the conservative well-posedness condition* (4) *holds. For any constant gain* $\bar{\alpha} > 0$ *and each constant input* $\nu \in \mathbb{R}^m$*, system* (46) *has a globally exponentially stable equilibrium point* $u = \breve{u} = \zeta(\nu)$ *with exponential decay rate proportional to* $\bar{\alpha}$*.*

Proof: First of all note that, due to the strict inequality in (4), there exists a small enough $\epsilon > 0$ such that $L - (1-\epsilon)I$ is Lyapunov Diagonally Stable.

Re-parametrize now time $s = \bar{\alpha} t$, so that, using $u' = \frac{du}{ds}$, (46) yields $u' = -u + L\,\mathrm{dz}_{[u^-,u^+]}(u) + \nu$. Following the steps at the beginning of the proof of [32, Thm 4], define $z = u - \breve{u} = u - \zeta(\nu)$, where ζ has been introduced in Proposition 1 and is well defined because (4) holds. Then, exploiting $L\,\mathrm{dz}_{[u^-,u^+]}(\zeta(\nu)) - \zeta(\nu) + \nu = 0$, we obtain

$$\begin{aligned} z' &= -(z + \zeta(\nu)) + L\,\mathrm{dz}_{[u^-,u^+]}(z + \zeta(\nu)) + \nu \\ &= -z + LG(z) \end{aligned} \tag{47}$$

$$G(z) := \mathrm{dz}_{[u^-,u^+]}(z + \zeta(\nu)) - \mathrm{dz}_{[u^-,u^+]}(\zeta(\nu)), \tag{48}$$

as in [32, eq. (12)]. The incremental $[0,1]$ sector properties of the deadzone function imply that function G in (48) belongs to the sector $[0,1]$. In particular, denoting by G_k the components of G, we have

$$0 \le \int_0^{z_i} G_k(\sigma) d\sigma \le |z_k|^2, \quad \forall k = 1, \dots, m. \tag{49}$$

Consider now dynamics (47) and, using the positive scalar ϵ introduced at the beginning of the proof, rewrite it as

$$z' = -\epsilon z - (1-\epsilon) z + LG(z) = -\epsilon z + f_z(z), \tag{50}$$

where $f_z(z)$ satisfies the assumptions of [32, Thm 4], selecting $\bar{G} = I$, $D = (1-\epsilon)I$ and $T = L$ with the notation of [32], because $L - (1-\epsilon)I$ is Lyapunov Diagonally Stable. Using the construction in [32, Thm 4], there exists a positive definite matrix P and positive scalars η_k, $k = 1, \dots, m$, such that the continuously differentiable function

$$Y(z) := z^\top P z + \sum_{k=1}^{m} \eta_k \int_0^{z_k} G_k(\sigma) d\sigma \tag{51}$$

satisfies

$$\langle \nabla Y(z), f_z(z) \rangle \le 0. \tag{52}$$

Using bounds (49) allows us to conclude that function Y in (51) enjoys the following upper and lower bounds

$$\underline{c}_Y \|z\|^2 \le Y(z) \le \bar{c}_Y \|z\|^2, \tag{53}$$

where $\underline{c}_Y = \lambda_{\min}(P)$ and $\bar{c}_Y = \lambda_{\max}(P) + \max_{k \in \{0,\dots,m\}} \eta_k$.

Consider now the following bound, where we use the sector $[0,1]$ properties of G:

$$\langle \nabla Y(z), -\epsilon z \rangle \le -2\epsilon z^\top P z - \epsilon \sum_{k=1}^{m} \eta_k G_k(z_i) z_i \tag{54}$$

$$\le -2\epsilon \lambda_{\min}(P) \|z\|^2. \tag{55}$$

Combining this last bound with (52) and (53) we obtain

$$Y'(z) \le -2\epsilon \lambda_{\min}(P) \|z\|^2 \le -2 \frac{\epsilon \lambda_{\min}(P)}{\bar{c}_Y} Y(z),$$

so that, going back to the standard derivative $\dot{V}$ with respect to $t = \bar{\alpha}^{-1} s$, we obtain

$$\dot{Y}(z) \le -2\bar{\alpha} \frac{\epsilon \lambda_{\min}(P)}{\bar{c}_Y} Y(z), \tag{56}$$

showing exponential convergence to zero of Y with speed of convergence proportional to $2\bar{\alpha}$. Exploiting bounds (53), the exponential decay proportional to $\bar{\alpha}$ is transferred to $z = u - \breve{u}$, thus completing the proof. ∎

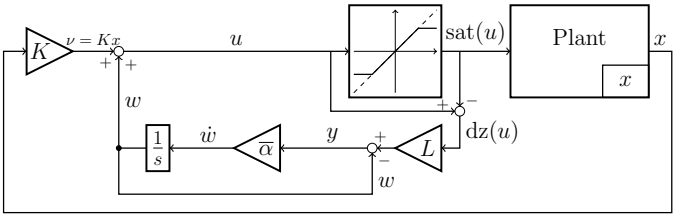

Fig. 7. Block diagram of the linear solution (57) to the dynamic problem.

Consider now the dynamic problem solved in Section IV via our novel nonlinear approach. As suggested in [15, Remark 9], the linear approach solves the same problem under the restrictive assumption (4). The proof of this fact was only sketched in [15, Remark 9]. Unfortunately, that sketch does not seem to lead to a viable proof path, even though the claimed result is correct. The proof path that we follow here is based on the developments of Sections III and IV and is a further contribution of this paper.

Inspired by (29), we rewrite the solution (12) as follows:

$$\begin{aligned}\dot{x} &= Ax + B\,\mathrm{sat}(Kx + w),\\ \dot{w} &= \bar{\alpha} y\\ y &= L\,\mathrm{dz}_{[u^-,u^+]}(u) - w,\end{aligned} \tag{57}$$

which corresponds to the block diagram shown in Figure 7. This scheme is evidently a linear version of the nonlinear scheme shown in Figure 6. Under the restrictive assumption (4), the following theorem parallels Theorem 2 and establishes the effectiveness of this solution.

Theorem 4. *Suppose that the conservative well-posedness condition* (4) *holds and there exist a Lyapunov function V and a scalar $c_v > 0$, such that $\|\nabla V(x)\| \le c_v\|x\|$, satisfying* (6)*,* (7) *for all $x \in \mathcal{E}(V,1)$ (respectively, globally), for the closed loop* (1)*,* (2)*.*

Then there exists $\alpha^* > 0$ such that, for any $\bar{\alpha} \ge \alpha^*$, the origin of the dynamically augmented implementation (57) *is* locally exponentially stable *with basin of attraction containing the set $\bar{\mathcal{E}}$ in* (31) *(respectively,* globally exponentially stable*).*

Proof: The proof follows similar steps to those in the proof of Theorem 2, by exploiting an extension of the function Y constructed in the proof of Theorem 3, to the case with $z := u - \breve{u}$, and $\breve{u} := \zeta(Kx)$, so that Y becomes indirectly also a function of x. In particular, using the same symbol Y with a slight abuse of notation, the function defined in (51) becomes (using dz in place of $\mathrm{dz}_{[u^-,u^+]}$ to simplify the notation)

$$\begin{aligned}Y(z,x) &:= z^\top P z\\ &+ \sum_{k=1}^{m} \eta_k \int_0^{z_k} [\mathrm{dz}(\sigma + \zeta_k(Kx)) - \mathrm{dz}(\zeta_k(Kx))]\,d\sigma\end{aligned} \tag{58}$$

The challenge in adapting the proof of Theorem 2 is that we need to establish suitable properties of the gradient of Y. In particular, first notice that, for almost all (x,z),

$$\begin{aligned}\|\nabla_z Y(z,x)\| &= \|2Pz + \mathrm{diag}(\eta)(\mathrm{dz}(z+\breve{u}) - \mathrm{dz}(\breve{u}))\|\\ &\le (2\|P\| + \|\eta\|)\|z\| =: c_{\nabla_z}\|z\|,\end{aligned} \tag{59}$$

where we used the 1-Lipschitz property of the deadzone function in the second line. For the gradient with respect to x, recalling that ζ is globally Lipschitz with Lipschitz constant ℓ_ζ, from (58) we get, for almost all (x,z),

$$\|\nabla_x Y(z,x)\| \le \sum_{k=1}^{m} \eta_k \int_0^{|z_k|} 2\ell_\zeta \|K\| d\sigma \le c_{\nabla_x}\|z\|, \tag{60}$$

where we used again the 1-Lipschitz property of the deadzone function, and where $c_{\nabla_x} := 2m\|\eta\|\ell_\zeta\|K\|$.

With the bounds (59) and (60) established above on the gradient of Y, let us now follow similar steps to the proof of Theorem 2 and, parallel to (32), consider $z := u - \breve{u}$, with $\breve{u} := \zeta(Kx)$ (where ζ is characterized in Proposition 1) and define

$$U(x,z) := V(x) + Y(z,x). \tag{61}$$

Using (6) and (53), function U satisfies

$$\underline{c}_U \left\|\left[\begin{smallmatrix}x\\ z\end{smallmatrix}\right]\right\|^2 \le U(x,z) \le \bar{c}_U \left\|\left[\begin{smallmatrix}x\\ z\end{smallmatrix}\right]\right\|^2, \tag{62}$$

for some positive scalars $\underline{c}_U, \bar{c}_U$. Then, with (35) and the left inequality in (34), we get

$$\dot{V}(x) \le -\mu\|x\|^2 + c_v\|B\|\|x\|\|z\|, \tag{63}$$

paralleling (35).

Consider now function Y in (58) and note that, exploiting (46), (47) and (53), inequality (56) can be written as

$$\begin{aligned}\langle \nabla_z Y(z,x), -z + L\,\mathrm{dz}_{[u^-,u^+]}(u) - L\,\mathrm{dz}_{[u^-,u^+]}(\breve{u})\rangle\\ \le -\bar{\alpha} c_Y \|z\|^2,\end{aligned} \tag{64}$$

with $c_Y := 2\frac{\epsilon\lambda_{\min}(P)\underline{c}_Y}{\bar{c}_Y}$. Proceeding as in (47) and exploiting $L\,\mathrm{dz}_{[u^-,u^+]}(\breve{u}) - \breve{u} + Kx = 0$, we may now write, using (57), and for almost all x (recall that $\breve{u} = \zeta(Kx)$),

$$\begin{aligned}\dot{z} &= \dot{u} - \dot{\breve{u}} = \bar{\alpha} y + K\dot{x} - \Delta_{\breve{u}} K\dot{x}\\ &= \bar{\alpha}(-z + L\,\mathrm{dz}_{[u^-,u^+]}(u) - L\,\mathrm{dz}_{[u^-,u^+]}(\breve{u})) + B_{\breve{u}}\dot{x},\end{aligned}$$

where $B_{\breve{u}} := K - \Delta_{\breve{u}} K$ satisfies $\|B_{\breve{u}} := K - \Delta_{\breve{u}} K\| \le \bar{b}$ for some positive scalar $\bar{b}$, due to the properties of $\Delta_{\breve{u}} \in \mathbf{\Delta}$, as per (3). With the above expression of $\dot{z}$, exploiting (34) and (36), we get from (64),

$$\begin{aligned}\langle \nabla_z Y(z,x), \dot{z}\rangle &\le -\bar{\alpha} c_Y\|z\|^2 + \|\nabla_z Y(z,x)\|\bar{b}\|\dot{x}\|\\ &\le -\bar{\alpha} c_Y\|z\|^2 + \bar{b}\; c_{\nabla_z}\|z\|(\theta\|x\| + \|B\|\|z\|),\end{aligned} \tag{65}$$

for almost all (x,z). We may proceed similarly for the gradient with respect to x by upper bounding $\|\dot{x}\|$ as in (65), to get from (60),

$$\begin{aligned}\langle \nabla_x Y(z,x), \dot{x}\rangle &\le \|\nabla_x Y(z,x)\|\|\dot{x}\|\\ &\le c_{\nabla_x}\|z\|(\theta\|x\| + \|B\|\|z\|),\end{aligned} \tag{66}$$

for almost all (x,z). The proof is then completed just as in the proof of Theorem 2 by

i) first combining bounds (63), (65) and (66) into a quadratic form involving $\left[\begin{smallmatrix}\|x\|\\ \|z\|\end{smallmatrix}\right]$, which can be made negative definite with a large enough $\bar{\alpha}$;

ii) then performing a swap between variables z and w in a similar way to what is done at the end of the proof of Theorem 2, which is possible due to the bounds in (25), establishing the equivalence between the error coordinates $\|y\|^2$ or $\|z\|^2 = \|u - \breve{u}\|^2$;

iii) finally applying Proposition 3 with $\mathcal{V}(x,w) := U(x, w + Kx - \zeta(Kx))$, paralleling again the proof of Theorem 2. ■

VI. Adaptive Selection of the Gain α

Theorems 2 and 4 both establish the existence of a large enough gain α^* ensuring (global) asymptotic stability, but determining such a gain, depending on the properties of the dynamics (1) and the gains K and L in the feedback loop, as represented by the Lyapunov function V, is challenging. The expression of α^* given in (39) contains constants whose value is typically unknown and provides an *extremely conservative* bound. While theoretically one could state that selecting very large values of $\bar{\alpha}$ in (29) or (57) is not problematic, undesired behaviors may emerge in practical implementations due to unmodeled dynamics, sampled-data implementations in real-time systems and similar robustness issues.

Due to this fact, inspired by the works in [42] and [43], we provide in this section an adaptive selection of α, which becomes a state of the extended dynamics, with the goal in mind of addressing situations where the value α^* is not known. In particular, we propose the following generalization of the dynamically augmented feedbacks (29) or (57),

$$\begin{aligned} \dot{x} &= Ax + B\,\mathrm{sat}(Kx + w), \\ \dot{w} &= -\alpha\Phi(y), \\ \dot{\alpha} &= \rho\ \mathrm{dz}_{[0,\varepsilon]}(V(x)), \qquad\qquad \alpha(0) \geq 0 \\ y &= -u + L\,\mathrm{dz}_{[u_i^-, u_i^+]}(u) + Kx, \end{aligned} \tag{67}$$

where $\rho > 0$ is an arbitrary adaptation gain governing the speed of the adaptation and function $\Phi(y)$ may either represent the nonlinear solution $\Phi(y) = \mathrm{dz}^\star(y)$ in (29) or the linear solution $\Phi(y) = y$ in (57).

The adaptive closed loop (67) enjoys a few useful properties. First of all, note that α is a non-decreasing function, which intuitively speaking is supposed to asymptotically reach a large enough value to ensure the decrease of function V. On the other hand, rather than forcing V to decrease to zero, we seek for a *practical* convergence property, deliberately stopping the adaptation (namely imposing $\dot{\alpha} = 0$) whenever $V(x) \leq \varepsilon$, so that the adaptive scheme is not sensitive to noise. In particular, ε should generally be tuned to be larger than the image of the measurement noise transformed through function V and the practical convergence properties established in the next theorem ensure that the plant state x asymptotically reaches the set

$$\mathcal{E}(V, \varepsilon) := \{x \in \mathbb{R}^n :\ V(x) \leq \varepsilon\}. \tag{68}$$

Remark 7. The control proposed in (67) falls in the class of λ-tracking control (in our case, ε plays the role of λ) discussed in the book [44], to which the reader is referred for further details, including a strategy, viable in the absence of noise, which does not consider any deadzone in the adaptation equation.

The following theorem provides convergence guarantees for the global case. While it is possible to provide restrictive conditions addressing the non-global case, those would require developing convoluted bounds on the initial value of the state (x, u, α) that would be of little practical interest.

Theorem 5. *Suppose that the algebraic loop* (2) *is well-posed and there exist a continuously differentiable Lyapunov function V and a scalar $c_v > 0$, such that $\|\nabla V(x)\| \leq c_v \|x\|$, satisfying* (6), (7) *for the closed loop* (1), (2).

Then, for any value of $\rho > 0$, given any initial condition $(x(0), u(0), \alpha(0)) \in \mathbb{R}^n \times \mathbb{R}^m \times \mathbb{R}_{\geq 0}$, the corresponding solution of (67) *is such that*

i) *x converges asymptotically to the set $\mathcal{E}(V, \varepsilon)$ in* (68)*;*
ii) *α converges asymptotically to a constant $\alpha_\infty \geq 0$.*

Proof: The proof is inspired by [43] and [42].

Proof of item ii). First note that α is uniformly continuous (with a bounded derivative) and non-decreasing, due to dynamics (67). Assume, to the end of establishing a contradiction, that $\lim_{t \to +\infty} \alpha(t) \to +\infty$.

This implies that there exists a time $t' \geq 0$ such that

$$\alpha(t) \geq \alpha^*, \quad \forall t \geq t',$$

and the main steps of the proof of Theorem 2 may be followed (for both the cases $\Phi(y) = \mathrm{dz}^\star(y)$ in (29) and $\Phi(y) = y$ in (57)) to obtain that function $U(x, y)$ converges exponentially to zero after time t'. As a consequence, there exists a time $\bar{t} \geq t'$ such that,

$$V(x(t)) \leq \varepsilon \quad \Rightarrow \quad \dot{\alpha}(t) = 0, \quad \forall t \geq \bar{t},$$

which clearly establishes a contradiction because $\alpha(t)$ cannot become unbounded. Since α is non-decreasing and bounded, then, from monotone convergence, it must converge asymptotically to its least upper bound α_∞.

Proof of item i). Let us first prove that, for any initial condition, the state x is bounded. For the specific global case addressed here, this step is simplified [4] by the assumption that (6), (7) hold globally, which implies global exponential stability. Then, due to [1], this implies that A is Hurwitz, therefore the x dynamics in (67) is BIBO stable and, due to the boundedness of sat, the state x is bounded.

From boundedness of x and continuous differentiability of V, we have that $t \mapsto V(x(t))$ is uniformly continuous, and so is $t \mapsto \dot{\alpha}(t) = \rho\ \mathrm{dz}_{[0,\varepsilon]}(V(x(t)))$, due to the Lipschitz properties of dz. As a consequence, the fact (proven above) that $t \mapsto \alpha(t)$ converges to α_∞ as $t \to \infty$, combined with Barbalat's lemma [45, Lemma 8.2], implies that $t \mapsto \dot{\alpha}(t)$ converges to zero. Equivalently, $t \mapsto \mathrm{dz}_{[0,\varepsilon]}(V(x(t)))$ converges to zero, namely x converges to $\mathcal{E}(V, \varepsilon)$, as to be proven. ■

VII. Simulation Examples

We illustrate the linear and nonlinear augmentations proposed in Sections IV, V and VI, corresponding to Theorems 2, 4 and 5, on a few examples taken from the literature. Since we already illustrated in Example 3 the situations where the linear solution of Section V fails to work, we focus here on examples where the sufficient condition (4) holds, so that both the linear and the nonlinear solutions can be comparatively applied. We choose small-dimensional examples for simplicity, even though the advantage of the proposed approach, compared to the lookup table one, is particularly significant when the number of control inputs is relatively large.

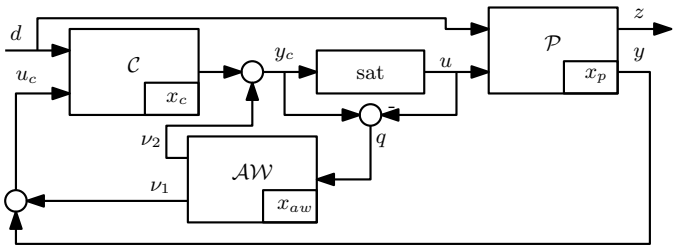

Fig. 8. Example 4: the external anti-windup augmentation scheme of [46] for a linear saturated plant $\mathcal{P}$ under the action of a linear controller $\mathcal{C}$ and of a linear dynamic external anti-windup filter $\mathcal{AW}$.

[4] In the non-global case, the boundedness of x should be concluded by a more involved argument contradicting boundedness of α by using radial unboundedness of V.

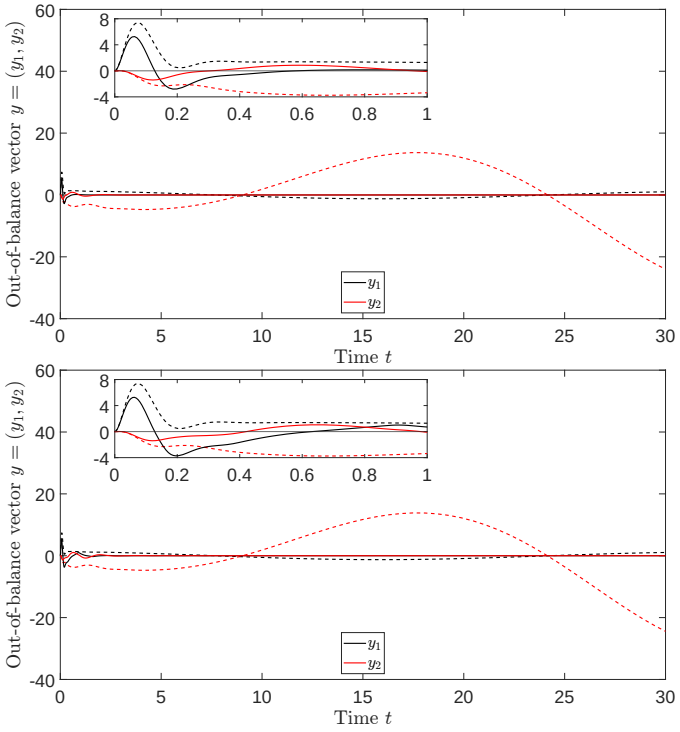

Fig. 9. Example 4. Out-of-balance vector y obtained when using the nonlinear solution (29), top, and the linear solution (57), bottom. The diverging solutions with $\bar{\alpha} = 0.01$ are dashed and the converging ones with $\bar{\alpha} = 10$ are solid.

Example 4. As a first example, let us consider the longitudinal dynamics of an F8 aircraft with a model first presented in [47] and then revisited in later works, such as [15] and [46]. We consider here the closed loop represented in [46, Figure 2], which is reported here in Figure 8 for the reader's convenience. According to the observations in Remark 3, since all the blocks of Figure 8 are linear (except for the saturation), then the overall scheme can be transformed into the scheme of Figure 1. For the numerical values of the quantities under consideration, the reader is referred to the reduced-order anti-windup selection described in [46, §5.2].

By construction, the algebraic loops arising from the designs in [46] (which use the same sector condition as the one used in our Proposition 2) guarantee the sufficient condition (4), therefore both the linear and the nonlinear solutions in (29) and (57) can be applied. Based on Theorems 2 and 4, for each one of these solutions, there exists $\alpha^\star$ such that, for $\bar{\alpha} \geq \alpha^\star$, the dynamically augmented feedback (29) or (57) is globally exponentially stable (this is because the original designs of [46] guarantee global exponential stability). We illustrate here the results obtained by implementing different values of $\bar{\alpha}$ with both our linear and nonlinear augmentations.

Figure 9 shows the out-of-balance vector y in (14a) for the nonlinearly augmented loop (29) (top) and the linearly augmented loop (57) (bottom). For both the linear and nonlinear cases, we run two sets of simulations. A first set (dashed lines) corresponds to the selection $\bar{\alpha} = 0.01$, which is smaller than $\alpha^\star$ and leads to diverging responses in both plots. A second set (solid lines) corresponds to the larger selection $\bar{\alpha} = 10$, which provide a graceful transient and desirable convergence in both cases. The two insets show the initial transient of the out-of-balance vector. With $\bar{\alpha} = 10$ (solid lines), we may observe a slightly more graceful transient for the nonlinear solution in this specific case. Nevertheless, the two approaches provide comparable desirable responses. ⋆

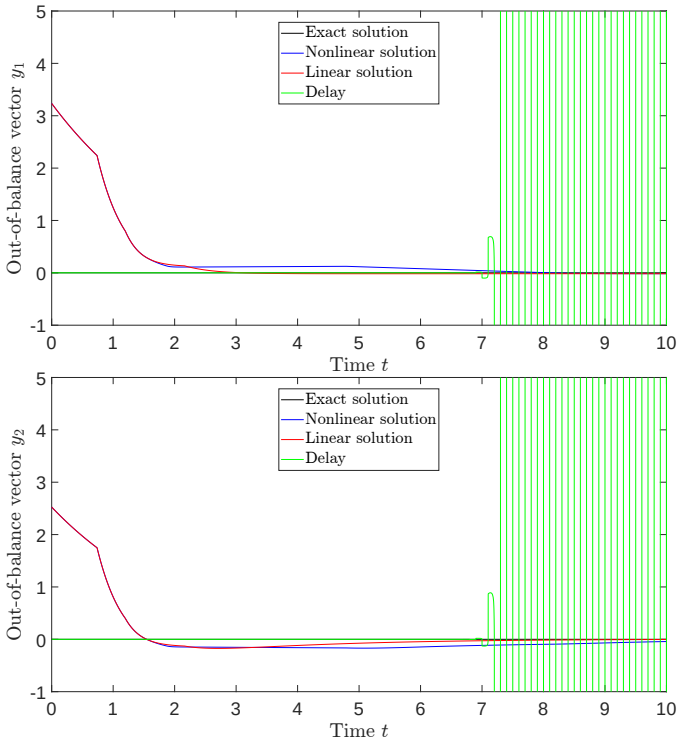

Fig. 10. Example 5. Out-of-balance vectors y when simulating the closed loop of [13, §5] with an unmodeled delay of 0.1 seconds in the algebraic loop (green). The linear (red) and nonlinear (blue) simulations both show asymptotic convergence to zero, while the exact solution (black) is associated with an identically zero response.

Example 5. The authors of [13] pointed out important fragility issues associated with the implementation of certain well-posed nonlinear algebraic loops wherein the Lipschitz constant of the explicit solution is excessively large (see also [48]). As a motivating example, [13, §5] discusses a specific feedback controller (initially introduced in [8]) where introducing an arbitrary small time delay in the algebraic loop has a destabilizing effect (see [13, Fig. 6, right]). We emphasize that the negative effect of this unmodeled delay confirms our discussions reported in Example 1, wherein an arbitrarily small delay can destabilize the feedback.

When focusing on that fragile example, our nonlinear and linear solutions of (29) and (57) provide desirable results, as expected from Theorems 2 and 4. For those two cases, the blue (nonlinear) and red (linear) curves reported in Figure 10 represent the out-of-balance vector y in (29) and (57), respectively as obtained when running our algorithm with $\bar{\alpha} = 0.5$ (similar curves are obtained for alternative selections of α). In the same figure, we report in black the results of a simulation performed by solving exactly the algebraic loop following the lookup table technique in [7, §2.3.7, item (3)], which corresponds

to $w = L\,\mathrm{dz}_{[u^-,u^+]}(u)$, therefore $y \equiv 0$. Finally, following [13, §5], we introduce a time delay of 0.1 seconds between $L\,\mathrm{dz}_{[u^-,u^+]}(u)$ and w, and the green curve represents the arising exponentially diverging evolution of the arising signal y, as per the last equation (29) and (57). ⋆

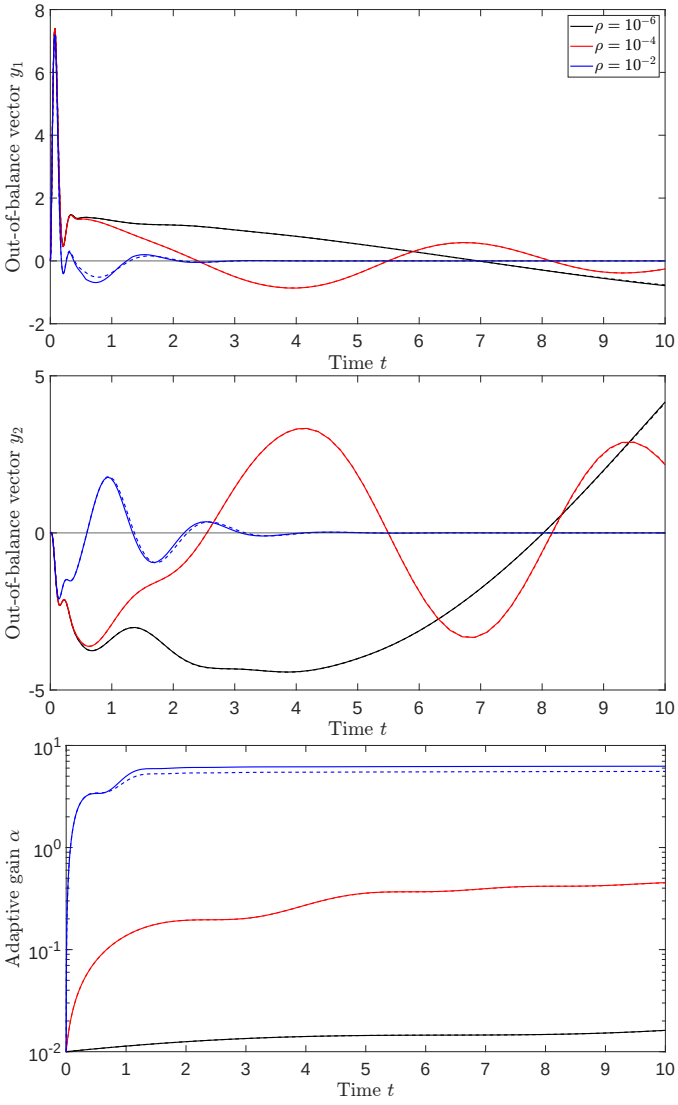

Fig. 11. Example 6. Adaptive algorithm (67) with the linear (dashed) and nonlinear (solid) solutions. The top plots represent the components of the out-of-balance vector y, while the bottom plot represents the adaptive gain α. Different colors represent different selections of parameter ρ.

Example 6. We illustrate in this example the adaptive approach of Section VI and, in particular, Theorem 5. To this end, we reconsider the system discussed in Example 4 (taken from [46]) where, instead of selecting a constant $\bar{\alpha}$, we implement the adaptive control law (67). Based on the simulations of Example 4 (see Figure 9), we expect the asymptotic value α_∞ of $\alpha(\cdot)$ (as characterized in Theorem 5) to be larger than the value $\bar{\alpha} = 0.01$ that led to instability in Figure 9. Since no explicit expression of the Lyapunov function certifying global exponential stability is given in [46], we apply the global condition at item (iii) of Proposition 2 and select function V in (67) as $V(x) := x^\top Q^{-1} x$, where Q is obtained by solving the LMIs (5) with $Y = 0$, yielding

$$Q^{-1} = \begin{bmatrix} 34.119 & 0.034299 & -273.25 & 300.42 \\ 0.034299 & 0.0027672 & -0.35325 & 0.37088 \\ -273.25 & -0.35325 & 2193.5 & -2410.4 \\ 300.42 & 0.37088 & -2410.4 & 2649.4 \end{bmatrix}.$$

We run simulations for both the nonlinear and the linear solutions (corresponding to (67) with $\Phi(y) = \mathrm{dz}^\star(y)$ and $\Phi(y) = y$, respectively) and we represent by dashed lines the linear ones and by solid lines the nonlinear ones. Figure 11 shows the simulation results for various values of ρ. The top two plots report the two components of the out-of-balance vector $y = (y_1, y_2)$, while the bottom plot shows the evolution of α in logarithmic scale (to ease comparison). Three values of ρ are tested in our simulations, corresponding to $\rho = 10^{-6}$ (black), $\rho = 10^{-4}$ (red) and $\rho = 10^{-2}$ (blue), while the value of ε in (67) has been set to 10^{-6}. The initial value of α is set to zero for all our simulations.

We emphasize that the closed-loop response is highly oscillatory in the initial "learning" phase, when α is too small and potentially associated with instability. Once α becomes large enough, the out-of-balance vector quickly converges to zero. Note also that the red and black curves have not reached their steady-state behavior at the end of the displayed simulation horizon $t = 10$. For each one of them, the adaptive gain α reaches the asymptotic values reported in Table I. Interestingly,

TABLE I
ASYMPTOTIC VALUES OF THE ADAPTIVE GAIN α IN EXAMPLE 6.

ρ	Linear solution $\Phi(y) = y$	Nonlinear solution $\Phi(y) = \mathrm{dz}^\star(y)$
10^{-6}	0.15152	0.15098
10^{-4}	0.48617	0.49356
10^{-2}	5.562	6.3398

for this specific example, the asymptotic value of α seems to be a monotonically increasing function of the gain ρ. Also note that all these asymptotic values are well below the value $\bar{\alpha} = 10$ used in Example 4. ⋆

VIII. CONCLUSIONS

In this paper we provided a comprehensive characterization of solutions to algebraic loops arising in control systems with saturations and deadzones. We presented a nonlinear scheme converging to the exact solution and allowing to preserve stability properties of algebraic-loop-based feedback controllers via dynamic augmentation. In addition to giving a nonlinear solution, whose effectiveness is rigorously proven whenever the algebraic loop is well-posed, we fully characterized the limits of an alternative intuitive approach, already suggested (without any proof) in the literature, and fully characterized the sufficient conditions under which the approach successfully solves the problem. Finally, since the ensuing constructions are based on the tuning of a large enough gain parameter, we discussed an adaptive implementation, based on high-gain adaptation. Simulation examples illustrated the relevance of our results and their relation with existing works.

REFERENCES

[1] E. Sontag, "An algebraic approach to bounded controllability of linear systems," *International Journal of Control*, vol. 39, no. 1, pp. 181–188, 1984.

[2] H. Sussmann, E. Sontag, and Y. Yang, "A general result on the stabilization of linear systems using bounded controls," *IEEE Transactions on Automatic Control*, vol. 39, no. 12, pp. 2411–2424, 1994.

[3] A. Teel, "Global stabilization and restricted tracking for multiple integrators with bounded controls," *Systems & Control Letters*, vol. 18, pp. 165–171, 1992.

[4] T. Hu and Z. Lin, *Control systems with actuator saturation: analysis and design*. Springer, 2001.

[5] Y. Li and Z. Lin, *Stability and performance of control systems with actuator saturation*. Springer, 2018.

[6] S. Tarbouriech, G. Garcia, J. Gomes da Silva Jr., and I. Queinnec, *Stability and stabilization of linear systems with saturating actuators*. Springer-Verlag London Ltd., 2011.

[7] L. Zaccarian and A. Teel, *Modern anti-windup synthesis: control augmentation for actuator saturation*. Princeton University Press, Princeton (NJ), 2011.

[8] E. F. Mulder, M. V. Kothare, and M. Morari, "Multivariable anti-windup controller synthesis using linear matrix inequalities," *Automatica*, vol. 37, pp. 1407–1416, 2001.

[9] J. Willems, *The analysis of feedback systems*. MIT Press, 1971.

[10] L. Zaccarian and A. Teel, "A common framework for anti-windup, bumpless transfer and reliable designs," *Automatica*, vol. 38, no. 10, pp. 1735–1744, 2002.

[11] A. Syaichu-Rohman, R. H. Middleton, and M. M. Seron, "A multivariable nonlinear algebraic loop as a QP with applications to MPC," in *2003 European Control Conference (ECC)*, November 2003, pp. 1–6.

[12] M. Soroush and K. Muske, "Analytical model predictive control," in *Nonlinear model predictive control*, F. Allgower and A. Zheng, Eds. Springer, 2000, ch. 9, pp. 163–179.

[13] A. Syaichu-Rohman and R. H. Middleton, "On the robustness of multivariable algebraic loops with sector nonlinearities," in *Proceedings of the IEEE Conference on Decision and Control*, vol. 1, 2002, pp. 1054–1059.

[14] G. Grimm, A. Teel, and L. Zaccarian, "Establishing Lipschitz properties of multivariable algebraic loops with incremental sector nonlinearities," in *IEEE International Conference on Decision and Control*, vol. 6, 2003, pp. 5667–5672.

[15] G. Grimm, J. Hatfield, I. Postlethwaite, A. R. Teel, M. C. Turner, and L. Zaccarian, "Antiwindup for stable linear systems with input saturation: an LMI-based synthesis," *IEEE Transactions on Automatic Control*, vol. 48, no. 9, pp. 1509–1525, 2003.

[16] G. Herrmann, M. Turner, and I. Postlethwaite, "Some new results on anti-windup-conditioning using the Weston-Postlethwaite approach," in *IEEE Conference on Decision and Control*, vol. 5, Dec. 2004, pp. 5047–5052.

[17] T. Hu, A. R. Teel, and L. Zaccarian, "Stability and performance for saturated systems via quadratic and nonquadratic Lyapunov functions," *IEEE Transactions on Automatic Control*, vol. 51, no. 11, pp. 1770–1786, 2006.

[18] G. Li, G. Herrmann, D. Stoten, J. Tu, and M. Turner, "A novel robust disturbance rejection anti-windup framework," *International Journal of Control*, vol. 84, no. 1, pp. 123–137, 2011.

[19] A. A. Adegbege and W. P. Heath, "A framework for multivariable algebraic loops in linear anti-windup implementations," *Automatica*, vol. 83, pp. 81–90, 2017.

[20] S. Mariano, F. Blanchini, S. Formentin, and L. Zaccarian, "Asymmetric state feedback for linear plants with asymmetric input saturation," *IEEE Control Systems Letters*, vol. 4, no. 3, pp. 608–613, 2020.

[21] G. Herrmann, B. Hredzak, M. Turner, I. Postlethwaite, and G. Guo, "Improvement of a novel dual-stage large-span track-seeking and track-following method using anti-windup compensation," in *Prof. of the American Control Conference*, 2006, pp. 1990–1997.

[22] A. Cristofaro, S. Galeani, S. Onori, and L. Zaccarian, "A switched and scheduled design for model recovery anti-windup of linear plants," *European Journal of Control*, vol. 46, pp. 23–35, 2019.

[23] D. Dai, T. Hu, A. Teel, and L. Zaccarian, "Output feedback design for saturated linear plants using deadzone loops," *Automatica*, vol. 45, no. 12, pp. 2917–2924, 2009.

[24] C. Duan and F. Wu, "Output-feedback control for switched linear systems subject to actuator saturation," *International journal of control*, vol. 85, no. 10, pp. 1532–1545, 2012.

[25] T. Hu, A. Teel, and L. Zaccarian, "Anti-windup synthesis for linear control systems with input saturation: achieving regional, nonlinear performance," *Automatica*, vol. 44, no. 2, pp. 512–519, 2008.

[26] S. Sajjadi-Kia and F. Jabbari, "Multi-stage anti-windup compensation for open-loop stable plants," *IEEE Transactions on Automatic Control*, vol. 56, no. 9, pp. 2166–2172, 2011.

[27] ——, "Modified dynamic anti-windup through deferral of activation," *International Journal of Robust and Nonlinear Control*, vol. 22, no. 15, pp. 1661–1673, 2012.

[28] X. Wu and Z. Lin, "Design of multiple anti-windup loops for multiple activations," *Science China Information Sciences*, vol. 55, no. 9, pp. 1925–1934, 2012.

[29] ——, "Dynamic anti-windup design in anticipation of actuator saturation," *International Journal of Robust and Nonlinear Control*, vol. 24, no. 2, pp. 295–312, 2014.

[30] C. Yuan and F. Wu, "Switching control of linear systems subject to asymmetric actuator saturation," *International Journal of Control*, vol. 88, no. 1, pp. 204–215, 2015.

[31] F. Blanchini, G. Fenu, G. Giordano, and F. A. Pellegrino, "Model-free plant tuning," *IEEE Transactions on Automatic Control*, vol. 62, no. 6, pp. 2623–2634, June 2017.

[32] M. Forti and A. Tesi, "New conditions for global stability of neural networks with application to linear and quadratic programming problems," *IEEE Transactions on Circuits and Systems I: Fundamental Theory and Applications*, vol. 42, no. 7, pp. 354–366, 1995.

[33] S. Nicosia, A. Tornambè, and P. Valigi, "A solution to the generalized problem of nonlinear map inversion," *Systems & control letters*, vol. 17, no. 5, pp. 383–394, 1991.

[34] S. Nicosia, A. Tornambè, and P. Valigi, "Nonlinear map inversion via state observers," *Circuits, Systems and Signal Processing*, vol. 13, no. 5, pp. 571–589, 1994.

[35] L. Menini, C. Possieri, and A. Tornambè, "Newton-like algorithms for the inversion of switched maps," *Automatica*, vol. 104, pp. 228–232, 2019.

[36] T. Mylvaganam, R. Ortega, J. Machado, and A. Astolfi, "Dynamic zero finding for algebraic equations," in *2018 European Control Conference*, 2018, pp. 1244–1249.

[37] J. M. G. da Silva and S. Tarbouriech, "Antiwindup design with guaranteed regions of stability: an LMI-based approach," *IEEE Transactions on Automatic Control*, vol. 50, no. 1, pp. 106–111, 2005.

[38] F. H. Clarke, Y. S. Ledyaev, R. J. Stern, and P. R. Wolenski, *Nonsmooth Analysis and Control Theory*, ser. Graduate Texts in Mathematics. New York: Springer-Verlag, 1998, vol. 178.

[39] D. G. Luenberger, *Optimization by Vector Space Methods*. John Wiley & Sons, 1990.

[40] A. Teel and L. Praly, "On assigning the derivative of a disturbance attenuation control Lyapunov function," *Mathematics of Control, Signals, and Systems (MCSS)*, vol. 13, no. 2, pp. 95–124, 2000.

[41] M. Della Rossa, R. Goebel, A. Tanwani, and L. Zaccarian, "Piecewise structure of Lyapunov functions and densely checked decrease conditions for hybrid systems," *Mathematics of Control, Signals, and Systems (MCSS), to appear*, 2021.

[42] F. Blanchini and E. Ryan, "A Razumikhin-type lemma for functional differential equations with application to adaptive control," *Automatica*, vol. 35, no. 5, pp. 809–818, 1999.

[43] F. Blanchini and P. Giannattasio, "Adaptive control of compressor surge instability," *Automatica*, vol. 38, no. 8, pp. 1373–1380, 2002.

[44] A. Ilchmann, *Non-identifier-based High-Gain Adaptive Control*, ser. Lecture Notes in Control and Information Sciences. Springer-Verlag, London, 1993, vol. 89.

[45] H. K. Khalil, *Nonlinear Systems*. Prentice Hall, 2002.

[46] S. Galeani, M. Massimetti, A. R. Teel, and L. Zaccarian, "Reduced order linear anti-windup augmentation for stable linear systems," *International Journal of Systems Science*, vol. 37, no. 2, pp. 115–127, 2006.

[47] P. Kapasouris, M. Athans, and G. Stein, "Design of feedback control systems for stable plants with saturating actuators," in *Proceedings of the 27th IEEE Conference on Decision and Control*, vol. 1, 1988, pp. 469–479.

[48] G. Grimm, A. R. Teel, and L. Zaccarian, "Results on linear LMI-based external anti-windup design," in *Proceedings of the 41st IEEE Conference on Decision and Control*, vol. 1, 2002, pp. 299–304.

Franco Blanchini (Senior Member, IEEE) is professor in Automatic Control and the Director of the Laboratory of System Dynamics at the University of Udine. He is co–author of the book "Set theoretic methods in control", Birkhäuser. He is the recipient of the 2001 ASME Oil & Gas Application Committee Best Paper Award and of the 2002 IFAC survey paper prize for the article "Set Invariance in Control – a survey", Automatica, November 1999 and the High Impact paper award for the same work. He has been an Associate Editor for Automatica, for IEEE Trans. on Automatic Control and Editor for IEEE CSS letters.

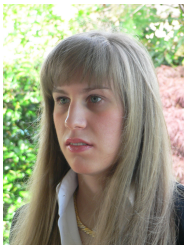

Giulia Giordano (Senior Member, IEEE) received her Ph.D. degree from the University of Udine, Italy, in 2016. She visited the California Institute of Technology, USA, in 2012, and the University of Stuttgart, Germany, in 2015. She was a Research Fellow at Lund University, Sweden, from 2016 to 2017, and an Assistant Professor at the Delft University of Technology, The Netherlands, from 2017 to 2019. She is currently an Assistant Professor at the University of Trento, Italy. She received the Outstanding Reviewer Letter from the IEEE Transactions on Automatic Control in 2016 and from the Annals of Internal Medicine in 2020; the EECI Ph.D. Award 2016; the NAHS Best Paper Prize 2017; and the SIAM Activity Group on Control and Systems Theory Prize 2021. Her main research interests are focused on dynamical networks and biological systems.

Francesco Riz received his M.Sc. in Mechatronics Engineering *cum laude* from the University of Trento, Italy in 2020. He is currently a PhD student in Mechatronics Engineering at that same university. His main research interests focus on the observability-based trajectory planning of multi-agent robotic systems.

Luca Zaccarian (Fellow, IEEE) received the Ph.D. degree in computer and control engineering from the University of Roma Tor Vergata (Italy) in 2000, respectively. From 2000 to 2011 he has been Assistant Professor and then Associate Professor at that same university. Since 2011 he is Directeur de Recherche at the LAAS-CNRS, Toulouse (France) and since 2013 he holds a part-time professor position at the University of Trento, Italy. Luca Zaccarian's main research interests include analysis and design of nonlinear and hybrid control systems, modeling and control of mechatronic systems. He was a recipient of the 2001 O. Hugo Schuck Best Paper Award given by the American Automatic Control Council.